ELSEVIER

Biochimica et Biophysica Acta 1559 (2002) 69–78

BIOCHIMICA ET BIOPHYSICA ACTA
BBA

www.bba-direct.com

Low-affinity Ca^{2+} and Ba^{2+} binding sites in the pore of α7 nicotinic acetylcholine receptors

L.K. Lyford [a], J.W. Lee [a,1], R.L. Rosenberg [a,b,*]

[a] *Department of Pharmacology, CB #7365, University of North Carolina at Chapel Hill, Chapel Hill, NC 27599, USA*
[b] *Department of Cell and Molecular Physiology, University of North Carolina at Chapel Hill, Chapel Hill, NC, USA*

Received 11 July 2001; received in revised form 9 October 2001; accepted 18 October 2001

Abstract

α7 nicotinic receptors are highly permeable to Ca^{2+} as well as monovalent cations. We extended the characterization of the Ca^{2+} permeation of non-desensitizing chick α7 receptors (S240T/L247T α7 nAChRs) expressed in *Xenopus* oocytes by (1) measuring the concentration dependence of conductance under conditions in which Ca^{2+} or Ba^{2+} were the only permeant cations in the extracellular solution, and (2) measuring the concentration dependence of Ca^{2+} block of K^+ currents through the receptors. The first set of experiments yielded an apparent affinity of 0.96 mM Ca^{2+} activity (2.4 mM concentration) for Ca^{2+} permeation and an apparent affinity of 0.65 mM Ba^{2+} activity (1.7 mM concentration) for Ba^{2+} permeation. The apparent affinity of Ca^{2+} inhibition of K^+ currents was 0.49 mM activity (1.5 mM concentration). The similarity of these apparent affinities in the millimolar range suggests that the pore of α7 receptors has one or more low-affinity Ca^{2+} binding sites and no high-affinity sites.

Keywords: Ion permeation; M2 domain; Planar lipid bilayer; Divalent cation; *Xenopus* oocyte

1. Introduction

Nicotinic acetylcholine receptors (nAChRs) are pentamers of homologous subunits surrounding a central cation-permeable pore [1]. Neuronal and muscle end-plate nicotinic receptors are relatively non-selective among monovalent cations, with permeability ratios (P_{Na}/P_K) of approximately 1.2 [2]. Neuronal nicotinic receptors are, however, more permeable to Ca^{2+} than muscle nAChRs [2–10]. In particular, α7 receptors (formed from the homomeric assembly of five α7 subunits) are the most Ca^{2+}-permeable of the neuronal nicotinic receptors [6,7,10,11]. The influx of Ca^{2+} through neuronal nicotinic receptors is important for their physiological functions of mediating fast synaptic transmission in the hippocampus [12,13], modulating excitatory and inhibitory neurotransmission [14], and regulating neuronal plasticity [13,15].

Previous studies have used changes in reversal potential to measure the selectivity of neuronal nicotinic receptors for Ca^{2+} [6–8,10] and fluorescence measurements of intracellular Ca^{2+} changes during receptor activation to measure the proportion of the inward current that is carried by Ca^{2+} ions [9,16,17]. These studies provide the evidence supporting the high Ca^{2+} permeability of neuronal nAChRs and indicate that a significant percentage of their current is carried by Ca^{2+}.

* Corresponding author. Fax: +1-919-966-5640.
E-mail address: bobr@med.unc.edu (R.L. Rosenberg).
[1] Present address: Memorial Sloan-Kettering Cancer Center, New York, NY 10021, USA.

0005-2736/02/$ – see front matter
PII: S0005-2736(01)00437-0

The goal of this study was to further characterize the permeation of Ca^{2+} through neuronal α7 nicotinic receptors by characterizing the interaction of Ca^{2+} with the pore. We used a non-desensitizing mutant of chick α7 receptors with a serine-to-threonine mutation at position 240 and a leucine-to-threonine mutation at position 247 (S240T/L247T α7 receptors) [18,19]. These receptors had permeation properties that were virtually identical to wild-type α7 receptors. More importantly, these receptors avoided the severe run-down problems reported for wild-type α7 receptors in excised patches [18,20] and permitted detailed permeation studies at the single-channel level. We took two complementary approaches. In one set of experiments, we measured the concentration dependence of Ca^{2+} permeation and thereby measured the apparent affinity with which Ca^{2+} interacted with the pore during Ca^{2+} permeation. In the other experiments, we evaluated the Ca^{2+}-dependent block of currents carried by K^+, and thereby determined the apparent affinity with which Ca^{2+} blocked monovalent cation currents. We found that both apparent affinities were approximately 0.5–1 mM Ca^{2+} activity (1–3 mM Ca^{2+} concentration), suggesting that the pore of α7 receptors is likely to have one or more low-affinity Ca^{2+} binding sites, no high-affinity sites, and, unlike voltage-gated Ca^{2+} channels, does not promote electrostatic repulsion between ions during permeation.

2. Materials and methods

2.1. Chemicals

(+)-Tubocurarine and $CaCl_2$ were obtained from Fluka (Milwaukee, WI, USA). QX-222 was obtained from Tocris Cookson (St. Louis, MO, USA). Gentamicin was obtained from Gibco-BRL (Gaithersburg, MD, USA). All other chemicals were from Sigma (St. Louis, MO, USA) or Fluka.

2.2. cDNAs, in vitro transcription, cRNA microinjections, and maintenance of Xenopus oocytes

The plasmid vectors, chick α7 cDNAs, mutagenesis, preparation of α7 cRNA, and the harvesting and maintenance of *Xenopus laevis* oocytes were described previously [19].

2.3. Two-electrode voltage clamp

Two-electrode voltage clamp was performed as described [19]. Oocytes were superfused in each recording solution for at least 4 min before applying ACh in that solution. Unless otherwise stated, oocytes were voltage-clamped at a constant holding potential of −60 mV.

Oocytes were injected with 46 nl of 50 mM BAPTA 15 min prior to recording to chelate intracellular Ca^{2+} and prevent the activation of Ca^{2+}-activated Cl^- channels [3]. The effectiveness of BAPTA in each oocyte was confirmed by comparing current–voltage (*I–V*) relationships obtained in Ca^{2+}-containing normal extracellular solution (96 mM NaCl, 2 mM KCl, 1 mM $MgCl_2$, 2.5 mM $CaCl_2$, and 10 mM Na-HEPES, pH 7.5) to *I–V* curves obtained in Ca^{2+}-free extracellular solution containing 1 mM EGTA instead of 2.5 mM $CaCl_2$. In Ca^{2+}-free extracellular solution, *I–V* curves displayed strong inward rectification. In normal extracellular solution in the absence of BAPTA injection, *I–V* curves were nearly linear due to outward current carried by the Ca^{2+}-activated Cl^- channels at positive voltages. In normal extracellular solution after BAPTA injection, *I–V* curves showed strong inward rectification, and were indistinguishable from those recorded in the absence of extracellular Ca^{2+}. Thus, strong inward rectification in normal extracellular solution was taken as evidence that the injected BAPTA was effective in chelating intracellular Ca^{2+}.

To obtain whole-cell *I–V* relationships of S240T/L247T α7 receptors, voltage steps from the −60 mV holding potential (10 mV intervals, 200 ms duration) were applied during the steady plateau of ACh-evoked current. Leak currents recorded in the absence of ACh were subtracted. To obtain whole-cell *I–V* relationships of wild-type α7 receptors (Fig. 1B,C), oocytes were voltage-clamped at the holding potential indicated, ACh was applied, and the peak ACh-evoked inward current was measured. Receptor run-down was adjusted by comparing the currents at each voltage to the currents at repeated measurements at −60 mV.

2.4. Permeability ratios

For measurements of divalent-over-monovalent selectivity, Ca-Na-MeS and Ba-Na-MeS solutions were used (90 mM NaOH, 2.5 mM KOH, 1 mM $Mg(OH)_2$, 10 mM HEPES, and methanesulfonic acid to pH 7.4). $Ca(OH)_2$ or $Ba(OH)_2$ (0–10 mM) was added before adjusting the pH with methanesulfonic acid [7]. The impermeant anion methanesulfonate (MeS^-) was used instead of chloride to further reduce any current through Ca^{2+}-activated Cl^- channels that remained after the BAPTA injection. The osmolarities of these solutions were similar to that of ND96. Reversal potentials were determined by interpolation of the *I–V* plots. Selectivity ratios were calculated from the shifts in reversal at different Ca^{2+} or Ba^{2+} concentrations [21] by the following equation:

$$P_{Ca}/P_{Na} = \frac{A_{Na^+,o}(1-e^{\Delta V_{rev}F/RT})}{4\,(A_{Ca^{2+},1})\,e^{\Delta V_{rev}F/RT}\,(1+e^{V_{rev,1}F/RT})^{-1} - 4\,(A_{Ca^{2+},2})\,(1+e^{V_{rev,2}F/RT})^{-1}}$$

where $A_{Ca^{2+},1}$ and $A_{Ca^{2+},2}$ are the activities of extracellular Ca^{2+} in the two conditions being compared (see below), $A_{Na^+,o}$ is the activity of Na^+, V_{rev} is the reversal potential, and *F*, *R*, and *T* have their usual meanings.

To measure the permeation of divalent cations in the absence of other permeant ions, currents were measured in Ca-NMG-MeS and Ba-NMG-MeS solutions (100 mM $MeSO_3$, 1 mM $MgSO_4$, 10 mM HEPES, and *N*-methyl-D-glucamine to pH 7.4) containing $Ca(OH)_2$ or $Ba(OH)_2$ (0–10 mM, added before adjusting the pH). In these solutions, the impermeant cation *N*-methylglucamine (NMG^+) replaced all permeant monovalent cations. The osmolarities of the solutions were similar to that of ND96. Slope conductances at the reversal potential were measured and were normalized to the slope conductance obtained in a Ca^{2+}-free normal extracellular solution (96 mM NaCl, 2 mM KCl, 1 mM $MgCl_2$, 1 mM EGTA, 10 mM Na-HEPES, pH 7.5). Leak currents recorded in the absence of ACh were subtracted.

2.5. Calcium activity

The activity of Ca^{2+} in different solutions was calculated as follows. Activity coefficients for $CaCl_2$ in mixtures of $CaCl_2$, NaCl, and KCl were obtained from Butler [22]. The activity coefficients for Ca^{2+} were estimated from the activity of $CaCl_2$ using Guggenheim's convention [22]: $\gamma_{Ca^{2+}} = (\gamma_{CaCl_2})^2$ where $\gamma_{Ca^{2+}}$ is the single ion activity coefficient of Ca^{2+}. For experiments where the anion species was MeS^-, the ion activities for Ba^{2+} and Ca^{2+} were obtained from Kielland [23].

2.6. Membrane vesicle preparations from *Xenopus* oocytes

The method for isolating membrane vesicles from *Xenopus* oocytes was based on a protocol by Perez et al. [24]. Briefly, oocytes were rinsed and homogenized in buffer A (200 mM KCl, 200 mM NaCl, and 5 mM PIPES, pH 6.8) containing 300 mM sucrose and the protease inhibitors 100 μM phenylmethylsulfonyl fluoride, 1 μM pepstatin, 1 μg/ml aprotinin, and 1 μg/ml leupeptin. The homogenate was layered onto a discontinuous sucrose gradient of 50% and 20% sucrose (0.75 ml each) in buffer A containing protease inhibitors. The gradient was centrifuged at $30\,000 \times g$ for 30 min in a TLS 55 rotor in a Beckman TL tabletop ultracentrifuge. The 20%:50% interface was collected, diluted three-fold with buffer A and pelleted at $50\,000 \times g$ for 30 min in a TLA 100.3 rotor. The membrane pellets were resuspended in buffer B (50 mM KCl, 50 mM NaCl, 300 mM sucrose, and 5 mM MOPS, pH 6.8), frozen in liquid nitrogen and stored at −70°C.

2.7. Single-channel recording of oocyte-expressed nAChRs reconstituted into planar lipid bilayers

Planar lipid bilayer recordings were performed as described [19] except that the lipid bilayers contained 8 mg/ml 1-palmitoyl-2-oleoyl phosphatidylethanolamine, 4 mg/ml 1-palmitoyl-2-oleoyl phosphatidylserine, and 8 mg/ml cholesterol (Avanti Polar Lipids, Alabaster, AL, USA). Voltages were assigned as *trans* relative to *cis*. The solutions contained 300 mM KCl, 0.5 mM $CaCl_2$, 10 mM HEPES, pH 7.0, and 20 μM ACh on the *cis* (extracellular) side, and 50 mM KCl, 50 mM NaCl, 10 mM HEPES, pH 7.0, and 20 μM ACh on the *trans* (intracellular) side. To promote fusion of vesicles to the planar lipid bilayer, 0.5 mM $CaCl_2$ was present on the *cis* side. ACh was

added to both chambers to activate nAChRs incorporated in either orientation (although all channels incorporated with their extracellular side facing the *cis* solution; see below). Membrane vesicles prepared from *Xenopus* oocytes expressing S240T/L247T α7 nAChRs were incorporated into the bilayers by applying them directly onto the *cis* face of the bilayer with a fire-polished glass probe [24]. Current amplitudes were calculated from Gaussian fits to amplitude histograms or from visual fitting of opening and closing transitions with computer-generated vectors.

3. Results

The goals of these experiments were to determine the properties of Ca^{2+} and Ba^{2+} selectivity and permeation of α7 nAChRs, and to measure the apparent affinity with which the divalent cations bind within the pore. We used a mutant receptor that has reduced desensitization properties, making it possible to perform single-channel studies in planar lipid bilayers where agonist is continually present. In addition, the slow desensitization improved the experiments in oocytes, where *I–V* measurements could

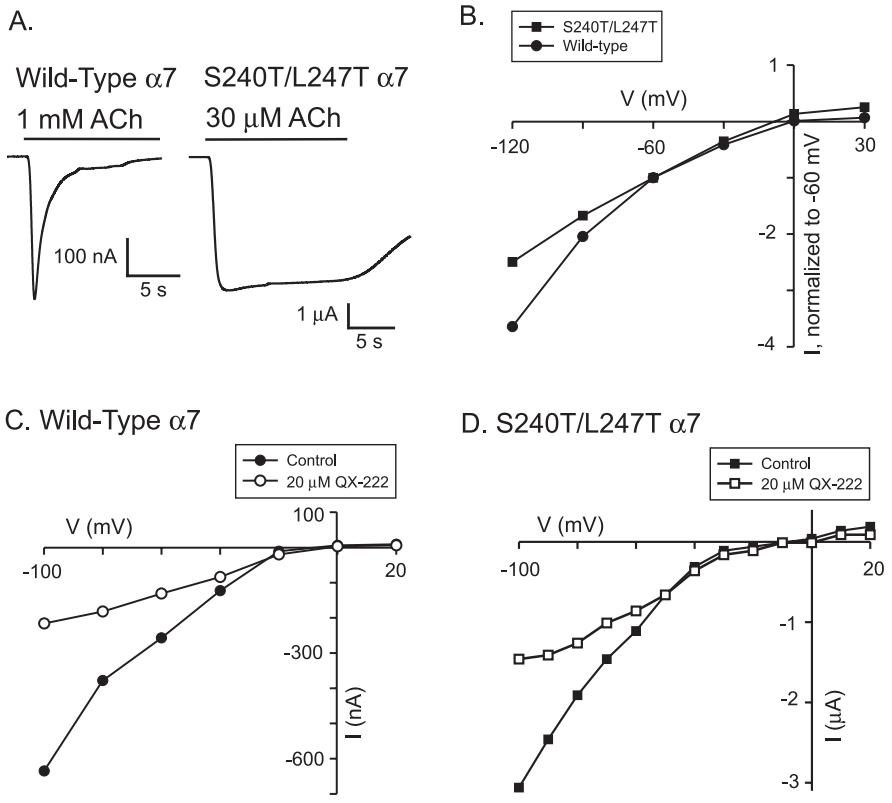

Fig. 1. S240T/L247T α7 nAChRs have pore properties that are similar to those of wild-type receptors. (A) Traces of ACh-evoked currents from wild-type (left) and S240T/L247T (right) α7 nAChRs recorded in normal extracellular solution. The ACh concentrations are those that gave maximal responses for each receptor (1 mM for wild-type, and 10 μM ACh for S240T/L247T α7 nAChRs). (B) Whole-cell *I–V* relationships of both wild-type and S240T/L247T α7 nAChRs display inward rectification in normal extracellular solution. Currents from both receptor types were evoked with maximal doses of ACh (same as in panel A) at the holding potentials indicated. To compare *I–V*s, the current amplitudes from each receptor type were normalized to the values obtained at −60 mV. The mean peak currents (±S.D.) at −60 mV were 0.15±0.09 μA ($n=6$, two batches) for wild-type α7 nAChRs and 4.0±2.1 μA ($n=4$, two batches) for S240T/L247T α7 nAChRs. (C,D) Both wild-type and S240T/L247T α7 nAChRs show voltage-dependent block by QX-222. *I–V* relationships for (C) wild-type and (D) S240T/L247T α7 nAChRs were generated in the presence (open symbols) and absence (closed symbols) of 20 μM QX-222. Currents were recorded in Ca^{2+}-free normal extracellular solution. Results are from single cells representative of three and six experiments with wild-type and mutant receptors, respectively. In panel C, the peak currents evoked by 300 μM ACh were determined at the holding potentials indicated. In panel D, 10 μM ACh was applied at a holding potential of −60 mV and the *I–V* relationship was obtained from a series of 10 mV voltage steps (−100 mV to 20 mV, 200 ms per step) applied during the steady plateau of inward current.

be made during a single sustained maximal inward current level, avoiding repeated applications of agonist and receptor run-down. The non-desensitizing receptor carried two mutations in the M2 pore-forming domain, a serine-to-threonine mutation (S240T) and a leucine-to-threonine mutation (L247T) [19]. This receptor was similar in its non-desensitizing properties to the L247T mutant characterized previously [18,25]. Fig. 1A shows current recordings of wild-type α7 nAChRs and the S240T/L247T α7 nAChRs, indicating the rapid desensitization kinetics of the wild-type nAChRs and the stable, long-lasting response of the S240T/L247T α7 nAChRs.

3.1. The S240T/L247T α7 nAChR and wild-type α7 nAChR have similar permeation properties

The permeation properties of S240T/L247T α7 nAChRs were similar to those of wild-type receptors in several important ways, indicating that the pores of S240T/L247T α7 receptors were very similar to those of wild-type receptors. We have shown previously that S240T/L247T nAChRs, like wild-type α7 nAChRs [8], are non-selective between Na^+ and K^+, with a P_{Na}/P_K of 1.2 [19]. In addition, both wild-type [7] and S240T/L247T α7 nAChRs [19] are highly permeable to Ca^{2+} (see below). The single-channel conductance of the mutant receptors (35 pS; see below) was similar to that of wild-type receptors in hippocampal neurons (38 pS [20]) and chick sympathetic neurons (35 pS [26]).

Fig. 1B–D provides additional critical evidence that the non-desensitizing S240T/L247T α7 receptor has ion permeation properties similar to those of wild-type α7 receptors. *I–V* relationships for both receptor types (Fig. 1B) show that both receptors display similar inward rectification. In addition, both the wild-type α7 nAChRs (Fig. 1C) [18] and the S240T/L247T α7 nAChRs (Fig. 1D) show similar voltage-dependent block by QX-222, an open-channel blocker that binds to residues in the pore-lining M2 domain [27]. This indicates that the overall pore geometry as probed by a pore-blocking molecule was not greatly affected by the S240T and L247T mutations. In summary, the non-desensitizing S240T/L247T nicotinic receptors had monovalent ion selectivity, single-channel conductance, Ca^{2+} permeability, inward rectification, and voltage-dependent block by QX-222 that were similar to those of wild-type receptors, and we conclude that the ion permeation pathway was not functionally affected by the S240T and L247T mutations.

3.2. Selectivity and apparent affinity of S240T/L247T α7 nAChRs for Ca^{2+}

To determine the selectivity of S240T/L247T α7 nAChRs for Ca^{2+} over Na^+, currents were recorded in solutions containing 90 mM Na^+ and varying concentrations of Ca^{2+} (Fig. 2) as described by Séguéla et al. [7] for wild-type α7 nAChRs. To reduce the activation of Ca^{2+}-activated Cl^- channels, oocytes were injected with BAPTA, a high-affinity Ca^{2+} chelator. In addition, Cl^- currents were minimized by replacing extracellular chloride with the impermeant anion MeS^-. Ba^{2+} currents were also measured because Ba^{2+} is less efficient than Ca^{2+} at activating Ca^{2+}-activated Cl^- channels [6] and has been commonly used as a Ca^{2+} substitute in studies of divalent ion permeation. Figs. 2A and 2B show *I–V* relationships in Ca-Na-MeS and Ba-Na-MeS, respectively. The reversal potentials from these data were plotted versus log Ca^{2+} activity (Fig. 2C) and log Ba^{2+} activity (Fig. 2D). The slopes of these plots were used to calculate a permeability ratio of Ca^{2+} to Na^+ (P_{Ca}/P_{Na}) of 43 and a P_{Ba}/P_{Na} of 4.1. The large positive E_{rev} value in 5.2 mM $A_{Ca^{2+}}$ (10 mM Ca^{2+} concentration; Fig. 2C) could have resulted from a large Ca^{2+} influx overwhelming the buffering ability of the injected BAPTA, resulting in some Ca^{2+}-activated Cl^- current. Thus P_{Ca}/P_{Na} may be somewhat overestimated. In comparison, wild-type rat α7 nAChRs expressed in oocytes are reported to have a P_{Ca}/P_{Na} of 6–20 [7,10] and a P_{Ba}/P_{Na} of 16.6 [6]. Taking into account the uncertainties regarding Ca^{2+}-activated Cl^- currents and the sensitivity of permeability ratios to small differences in reversal potentials, our results suggest that S240T/L247T α7 nAChRs had Ca^{2+} and Ba^{2+} selectivity in the same range as wild-type α7 nAChRs.

To determine the apparent affinity of binding sites within the pore for Ca^{2+} and Ba^{2+}, conductances were determined at different Ca^{2+} and Ba^{2+} concentrations in the absence of other permeant ions. In these experiments, Na^+ was replaced with NMG^+, a large impermeant cation. As described above, Cl^-

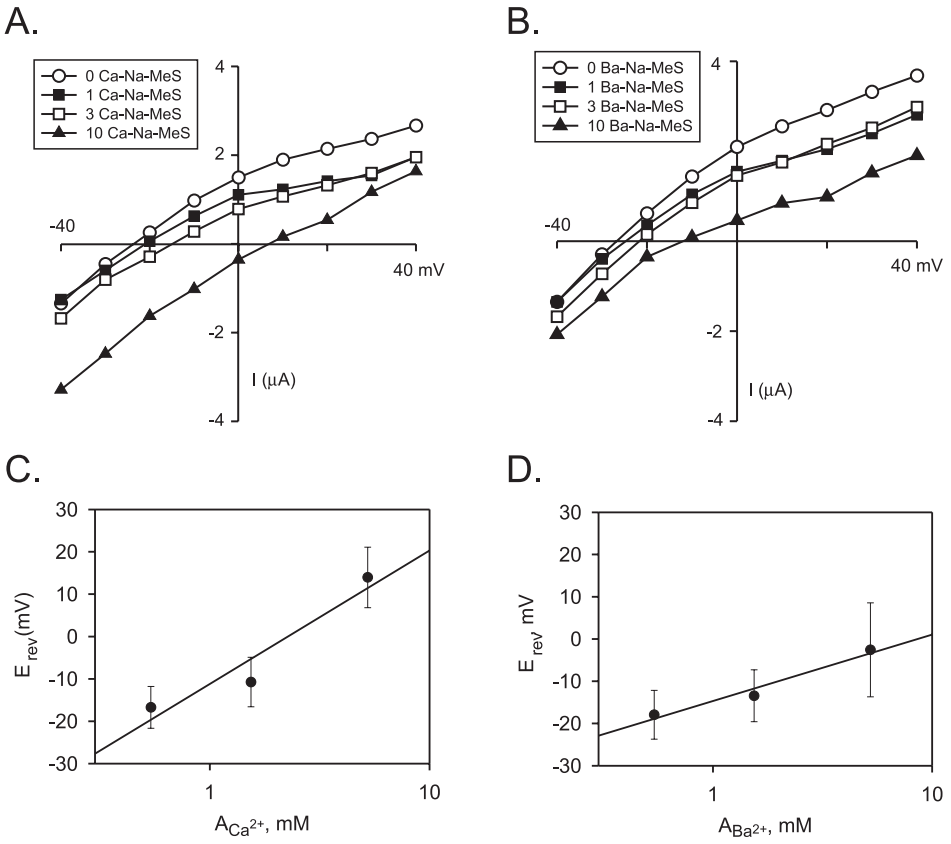

Fig. 2. Selectivity of S240T/L247T α7 nAChRs for Ca^{2+} and Ba^{2+} over Na^{+}. Currents were evoked by 100 μM ACh in (A) Ca-Na-MeS and (B) Ba-Na-MeS solutions containing concentrations of Ca^{2+} or Ba^{2+} ranging from 0 mM to 10 mM (as indicated in the figure). Representative data are shown from single cells. The reversal potentials were plotted versus (C) log $A_{Ca^{2+}}$ ($n=4$) and (D) log $A_{Ba^{2+}}$ ($n=4$).

was replaced with MeS^{-} and oocytes were injected with BAPTA to minimize the contribution of Ca^{2+}-activated Cl^{-} channels. Fig. 3 shows *I–V* plots of ACh-evoked responses in the presence of different concentrations of Ca^{2+} (Fig. 3A) or Ba^{2+} (Fig. 3B) as the only permeant ion. To determine the apparent affinity of divalent cations for the pore, the slope conductance at the reversal potential was measured from each curve, normalized by the conductance measured in a Ca^{2+}-free normal extracellular solution, and plotted versus Ca^{2+} or Ba^{2+} activity (Fig. 3C,D, respectively). The data were fitted with the Michaelis–Menten equation ($G = G_{max}/[1+K_m/A_{X^{2+}}]$), yielding apparent affinity constants of 0.96 mM $A_{Ca^{2+}}$ (2.4 mM Ca^{2+} concentration) and 0.65 mM $A_{Ba^{2+}}$ (1.7 mM Ba^{2+} concentration).

3.3. *Affinity of divalents measured from block of monovalent currents*

The conductance versus activity relationships indicate that Ca^{2+} and Ba^{2+} interact with the pore of α7 nAChRs with low affinity during the permeation process. However, the interaction of multiple ions within a pore during permeation can give the appearance of low-affinity interaction from conductance–activity plots, even when the individual ion binding sites have very high affinity [28,29]. For example, L-type Ca channels have a high-affinity binding site for Ca^{2+} block of monovalent currents with a K_d of ~1 μM [29,30], but because of multiple-ion interactions during Ca^{2+} permeation, the conductance–activity relationships suggest a K_m of 14 mM [31]. To test for the presence of high-affinity Ca^{2+} binding sites, we examined the affinity with which divalent ions

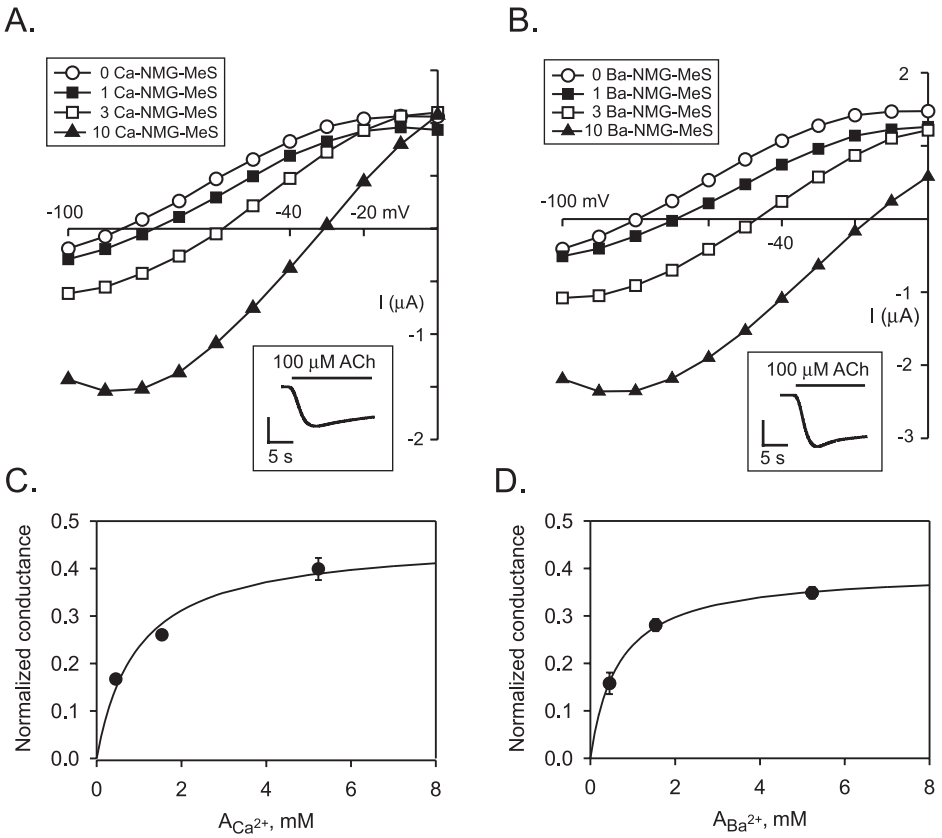

Fig. 3. S240T/L247T α7 nAChRs conduct Ca^{2+} and Ba^{2+} with apparent affinities of 0.96 mM and 0.65 mM (ion activity), respectively. Currents were evoked by 100 μM ACh in (A) Ca-NMG-MeS or (B) Ba-NMG-MeS in which the divalent cation was the only permeant ion. Insets show ACh-evoked currents in (A) 10 mM Ca^{2+} or (B) 10 mM Ba^{2+} at a holding potential of −60 mV (scale bars are 1 μA and 5 s in both panels). The data shown are representative of those obtained from seven or eight oocytes (A or B, respectively). Panels C and D show saturation isotherms for ACh-evoked currents of S240T/L247T α7 nAChRs in Ca^{2+} and Ba^{2+}, respectively. The slope conductances from *I–V* plots were measured at the reversal potentials and were plotted versus $A_{Ca^{2+}}$ or $A_{Ba^{2+}}$. To pool data from the oocytes, the slope conductances from each cell were normalized to the conductance at E_{rev} obtained in Ca^{2+}-free normal extracellular solution. The solid line represents the fit of the data to the equation: $G = G_{max}/(1+K_m/A_{X^{2+}})$, where G_{max} is the maximum normalized conductance, K_m is the half-maximal Ca^{2+} concentration (apparent affinity constant), and $A_{X^{2+}}$ and is the activity of Ca^{2+} or Ba^{2+}. The maximum normalized conductance for Ca^{2+} was 0.46 and the K_m was 0.96 mM $A_{Ca^{2+}}$ (2.4 mM Ca^{2+} concentration) ($n = 7$, two batches). The maximum normalized conductance for Ba^{2+} was 0.39 and the K_m was 0.65 mM $A_{Ba^{2+}}$ (1.7 mM Ba^{2+} concentration) ($n = 8$, two batches).

inhibited the flux of permeant monovalent cations. To pursue this set of experiments, S240T/L247T α7 nAChRs were expressed in *Xenopus* oocytes, and membrane vesicles from the oocytes were reconstituted into planar lipid bilayers (see Section 2). The main advantages of this approach are: (1) channels are studied at the single-channel level, so that conductance measurements are not contaminated by changes in channel gating [3,5], (2) the contributions of other ion channels are eliminated by selecting bilayers that contain only the nAChR channel, and (3) both the intracellular and extracellular solutions can be manipulated precisely.

To verify that the channels were nicotinic receptors, and to determine the orientation of the receptors in the bilayer, the reconstituted channels were tested with the nicotinic antagonists tubocurarine (TC; 4.4 μM) and hexamethonium (Hex; 100 μM). TC and Hex dramatically reduced the single-channel open times and apparent current amplitudes, respectively, in a reversible manner on the *cis* but not the *trans* side (data not shown). Thus, because TC com-

petes for ACh at the agonist binding site located on the extracellular, N-terminal domain [32], the channels were incorporated into the bilayers with their extracellular surface facing the *cis* chamber. In addition, the block by Hex and TC confirms the channels' nicotinic nature; both Hex and TC block ACh-evoked currents in oocytes expressing S240T/L247T α7 nAChRs (data not shown).

Previous studies have shown that extracellular Ca^{2+} reduces the unitary conductance of other (non-α7) neuronal nAChRs [5,33,34]. However, block of α7 nAChRs by intracellular Ca^{2+} has not been examined at the single-channel level. Thus, unitary currents of reconstituted S240T/L247T α7 nAChRs were measured in the presence of varying concentrations of *trans* Ca^{2+} (Fig. 4). As the concentration of Ca^{2+} was increased, the unitary currents at −60 mV were reduced (Fig. 4A). The unitary conductance decreased from 52 to 19 pS as the Ca^{2+} concentration increased from 0.5 to 20 mM (Fig. 4B).

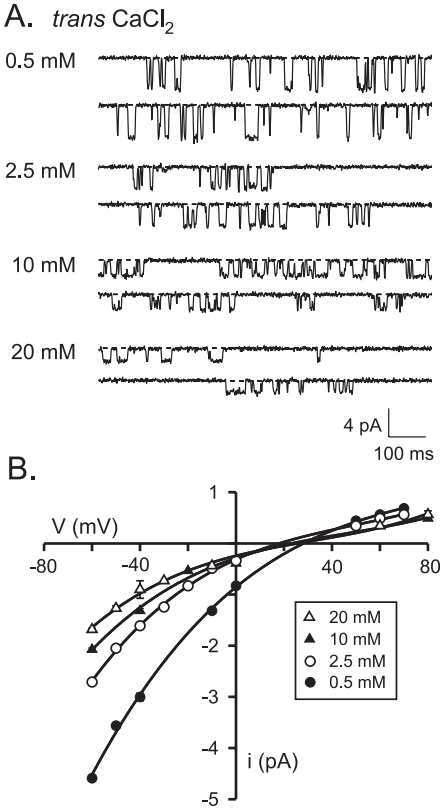

Fig. 4. Intracellular Ca^{2+} blocks unitary K^+ current. (A) Single-channel currents from S240T/L247T α7 nAChRs incorporated in planar lipid bilayers. The concentrations of $CaCl_2$ on the *trans* side are indicated in the figure. The holding potential was −60 mV for all traces (*trans* relative to *cis*), and downward transitions (channel openings) represent current flow from *cis* to *trans*. (B) Single-channel *I–V* relationships recorded at different Ca^{2+} concentrations.

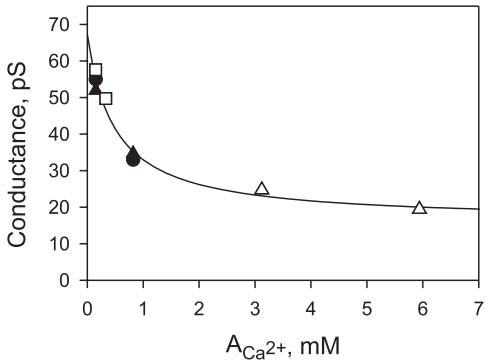

Fig. 5. Block of unitary conductance by Ca^{2+} activity has an apparent affinity (K_i) that is similar to the K_m for Ca^{2+} permeation. Chord conductances at −60 mV were plotted versus the activity of Ca^{2+} indicated. Each symbol shape represents a different experiment. Filled symbols indicate that Ca^{2+} concentrations were raised equally on both sides of the bilayer and open symbols represent changes in *trans* Ca^{2+} only. The data were fit to the equation $\gamma = \gamma_{min} + (\gamma_{max} - \gamma_{min})/(1 + A_{Ca^{2+}}/K_i)$, where γ_{max} and γ_{min} are the maximum and minimum conductances (67 and 16 pS, respectively), and K_i is the half-maximal inhibitory concentration. The K_i was 0.49 mM $A_{Ca^{2+}}$ (1.5 mM Ca^{2+} concentration).

To determine the affinity of the intracellular blocking site, the unitary chord conductance at −60 mV was plotted versus the activity of Ca^{2+} (Fig. 5). The IC_{50} for Ca^{2+} inhibition of monovalent currents was 0.49 mM $A_{Ca^{2+}}$ (1.5 mM Ca^{2+} concentration). This value was similar to the apparent affinity of Ca^{2+} during permeation (K_m) determined in Fig. 3C. Thus, these data are consistent with the hypothesis that the α7 nAChR has one or more low-affinity Ca^{2+} binding sites. The data also indicate that the pore of α7 nAChRs does not have a high-affinity Ca^{2+} binding site and does not promote the dramatic ion–ion interactions observed in L-type Ca channel permeation [28,29].

4. Discussion

This paper demonstrates that the pore of S240T/L247T α7 nAChRs contains one or more low-affinity

Ca^{2+} binding sites (with binding constants of 0.5–1 mM) and no high-affinity sites. We found that the apparent affinity for Ca^{2+} permeation was 0.96 mM Ca^{2+} activity (2.4 mM Ca^{2+} concentration), which is reasonably close to the apparent affinity for Ca^{2+}-dependent block of K^+ current of 0.49 mM Ca^{2+} activity (1.5 mM concentration).

Although the S240T/L247T α7 nicotinic receptors utilized in this study had two mutations in the pore-lining domain, many lines of evidence indicate that the pores of the mutant nicotinic receptors are functionally similar to those of wild-type α7 receptors: (1) both wild-type and L247T/S240T receptors have similar single-channel conductances of 35–38 pS (in the presence of 2–2.5 mM Ca^{2+}) (Figs. 4 and 5) [20,26]; (2) both receptors have similar selectivity for Ca^{2+} over monovalent cations (Fig. 2) [7,10]; (3) both receptors show similar degrees of inward rectification (Fig. 1B); (4) QX-222, which blocks nicotinic receptors by interacting with the pore, shows similar voltage-dependent block of both wild-type and L247T/S240T receptors (Fig. 1C,D); and (5) both receptors show similar lack of selectivity between Na^+ and K^+ ($P_{Na}/P_K \approx 1.2$) [2,19]. Previous single-channel studies with wild-type α7 nAChRs were limited by the severe run-down of activity in the excised patch configuration which allows multiple solutions to be readily tested [18,20].

Several previous reports have shown that α7 nicotinic receptors have a high selectivity for Ca^{2+} or Ba^{2+} over monovalent cations [6,7,10] and that Ca^{2+} flux through these receptors is large enough to increase intracellular Ca^{2+} [9,11,16,17,25]. However, to our knowledge this is the first study to measure the affinity of divalent ion interactions with the pore of α7 nicotinic receptors by measuring the concentration dependence of Ca^{2+} or Ba^{2+} permeation and the concentration dependence of Ca^{2+} block of monovalent currents.

Although α7 nAChRs are selective for Ca^{2+}, they are significantly different from voltage-gated Ca^{2+} channels that are exquisitely selective for Ca^{2+} over monovalent cations, with P_{Ca}/P_{Na} of ~1000 [28]. L-type Ca channels have a K_m for Ca^{2+} permeation of 14 mM (concentration) [31], but monovalent currents through these channels are blocked by Ca^{2+} with a K_i of ~1 μM [29,30]. The large difference between the K_m for Ca^{2+} permeation and the K_i for Ca^{2+} block of monovalent currents of L-type Ca channels is probably due to the existence of a single high-affinity Ca^{2+} binding site in the pore (with a K_d for Ca^{2+} binding of ~1 μM) that can interact simultaneously with two Ca^{2+} ions during Ca^{2+} permeation [29]. Electrostatic repulsion between the two Ca^{2+} ions is likely responsible for the rapid flux of ions through the pore [29]. α7 receptors, however, have a K_m for Ca^{2+} permeation of 2.4 mM (concentration), and a K_i for block of monovalent currents by Ca^{2+} of 1.5 mM (concentration). The similarity of these two values suggests that the pore of α7 receptors contains one (or more) low-affinity Ca^{2+} binding sites that do not promote ion repulsion in the pore. Thus, the pore of the α7 nicotinic receptor is functionally very different from that of highly selective voltage-gated Ca^{2+} channels.

Negatively charged membranes, including phosphatidylserine-containing bilayers used in these studies, have a surface potential that can increase the concentrations of cations at the membrane surface. In addition, fixed negative charges within the pore of the channel can have large effects on local concentrations of both monovalent and divalent cations at the mouth of the pore [35]. In principle, increased screening of these surface and fixed charges by the addition of Ca^{2+} could reduce the local concentration of permeating K^+, producing a Ca^{2+}-dependent reduction in channel conductance. This explanation is insufficient, however, because the effects of surface charge are limited to a layer approximately 8–9 Å from the charged surface [35]. The outer mouth of the AChR pore is 65 Å away from the extracellular membrane surface, and the inner mouth is 15 Å away from the intracellular surface [36]. Thus, screening of lipid surface charge is unlikely to be the cause of the observed Ca^{2+}-dependent decrease in unitary conductance. Fixed charges in the pore are likely to increase the local concentrations of Ca^{2+} and monovalent cations at the mouth of the pore [35], but these charges are expected to have a similar effects on the local concentration of Ca^{2+} during both Ca^{2+} permeation and Ca^{2+}-dependent block of monovalent permeation. Thus, our key observation – that the apparent affinities for Ca^{2+} permeation and Ca^{2+} block are approximately equal – is not affected by the presence of fixed charges.

The flux of Ca^{2+} through α7 nicotinic receptors

plays an essential role in their physiological functions [12–15]. The rapid flux of Ca^{2+} through the pore is assisted by the low affinity with which the ion binds during transit. The low affinity of Ca^{2+} binding is accompanied by a fairly low selectivity ($\sim$20) [6,7], but for these channels the high flux of Ca^{2+} even with modest selectivity is sufficient to cause significant elevation of intracellular Ca^{2+} [9,11,16,17].

Acknowledgements

We thank Susan Holley for excellent technical assistance, M. Ballivet (University of Geneva) for the α7 nAChR cDNA, and C. Labarca (California Institute of Technology) for the S240T/L247T α7 nAChR cDNA and pAMV vector. This work was supported by NIH Grant NS37317.

References

[1] N. Unwin, J. Struct. Biol. 121 (1998) 181–190.
[2] T.J. Nutter, D.J. Adams, J. Gen. Physiol. 105 (1995) 701–723.
[3] S. Vernino, M. Amador, C.W. Luetje, J.W. Patrick, J.A. Dani, Neuron 8 (1992) 127–134.
[4] C. Mulle, D. Choquet, H. Korn, J.-P. Changeux, Neuron 8 (1992) 135–143.
[5] C. Mulle, C. Léna, J.-P. Changeux, Neuron 8 (1992) 937–945.
[6] S.B. Sands, A.C.S. Costa, J.W. Patrick, Biophys. J. 65 (1993) 2614–2621.
[7] P. Séguéla, J. Wadiche, K. Dineley-Miller, J.A. Dani, J.W. Patrick, J. Neurosci. 13 (1993) 596–604.
[8] D. Bertrand, J.L. Galzi, A. Devillers-Thiéry, S. Bertrand, J.-P. Changeux, Proc. Natl. Acad. Sci. USA 90 (1993) 6971–6975.
[9] M. Rogers, J.A. Dani, Biophys. J. 68 (1995) 501–506.
[10] N.G. Castro, E.X. Albuquerque, Biophys. J. 68 (1995) 516–524.
[11] O. Delbono, M. Gopalakrishnan, M. Renganathan, L.M. Monteggia, M.L. Messi, J.P. Sullivan, J. Pharmacol. Exp. Ther. 280 (1997) 428–438.
[12] S. Jones, S. Sudweeks, J. Yakel, Trends Neurosci. 22 (1999) 555–561.
[13] R.S. Broide, F.M. Leslie, Mol. Neurobiol. 20 (1999) 1–16.
[14] A.B. MacDermott, L.W. Role, S.A. Siegelbaum, Annu. Rev. Neurosci. 22 (1999) 443–485.
[15] L.W. Role, D.K. Berg, Neuron 16 (1996) 1077–1085.
[16] Z. Zhou, E. Neher, Pflügers Arch. 425 (1993) 511–517.
[17] S. Vernino, M. Rogers, K.A. Radcliffe, J.A. Dani, J. Neurosci. 14 (1994) 5514–5524.
[18] F. Revah, D. Bertrand, J.-L. Galzi, A. Devillers-Thiéry, C. Mulle, N. Hussy, S. Bertrand, M. Ballivet, J.-P. Changeux, Nature 353 (1991) 846–849.
[19] L.K. Lyford, R.L. Rosenberg, J. Biol. Chem. 274 (1999) 25675–25681.
[20] Z. Shao, J. Yakel, J. Physiol. 527 (2000) 507–513.
[21] D. Ragozzino, B. Barabino, S. Fucile, F. Eusebi, J. Physiol. 507 (1998) 749–757.
[22] J.N. Butler, Biophys. J. 8 (1968) 1426–1433.
[23] J. Kielland, J. Am. Chem. Soc. 59 (1937) 1675–1678.
[24] G. Perez, A. Lagrutta, J.P. Adelman, L. Toro, Biophys. J. 66 (1994) 1022–1027.
[25] S. Fucile, E. Palma, A.M. Mileo, R. Miledi, F. Eusebi, Proc. Natl. Acad. Sci. USA 97 (2000) 3643–3648.
[26] C.R. Yu, L.W. Role, J. Physiol. 509 (1998) 651–656.
[27] P. Charnet, C. Labarca, R.J. Leonard, N.J. Vogelaar, L. Czyzyk, A. Gouin, N. Davidson, H.A. Lester, Neuron 4 (1990) 87–95.
[28] R.W. Tsien, P. Hess, E.W. McCleskey, R.L. Rosenberg, Annu. Rev. Biophys. Biophys. Chem. 16 (1987) 265–290.
[29] J. Yang, P.T. Ellinor, W.A. Sather, J.-F. Zhang, R.W. Tsien, Nature 366 (1993) 158–161.
[30] L. Parent, M. Gopalakrishnan, Biophys. J. 69 (1995) 1801–1813.
[31] P. Hess, J.B. Lansman, R.W. Tsien, J. Gen. Physiol. 88 (1986) 293–319.
[32] H.R. Arias, Brain Res. Rev. 25 (1997) 133–191.
[33] A. Mathie, S.G. Cull-Candy, D. Colquhoun, Proc. R. Soc. Lond. B. 232 (1987) 239–248.
[34] A. Mathie, S.G. Cull-Candy, D. Colquhoun, J. Physiol. 439 (1991) 717–750.
[35] B. Hille, Ion Channels of Excitable Membranes, 3rd edn., Sinauer Associates, Sunderland, MA, 2001, pp. 646–656.
[36] N. Unwin, J. Mol. Biol. 229 (1993) 1101–1124.